Published in final edited form as:
Nat Chem. ; 4(1): 26–30. doi:10.1038/nchem.1180.

Combining acid-base, redox and substrate binding functionalities to give a complete model for the [FeFe]-hydrogenase

James M. Camara and **Thomas B. Rauchfuss***
School of Chemical Sciences, University of Illinois, Urbana, Illinois 61801, USA

Abstract

Some enzymes function by coupling substrate turnover with electron transfer from a redox cofactor such as ferredoxin. In the [FeFe]-hydrogenases, nature's fastest catalysts for the production and oxidation of H_2, the one-electron redox by a ferredoxin complements the one-electron redox by the diiron active site. In this Article, we replicate the function of the ferredoxins with the redox-active ligand Cp*Fe($C_5Me_4CH_2PEt_2$) (*FcP**). *FcP** oxidizes at mild potentials, in contrast to most ferrocene-based ligands, which suggests that it might be a useful mimic of ferredoxin cofactors. The specific model is $Fe_2[(SCH_2)_2NBn](CO)_3$(*FcP**)(dppv) (1), which contains the three functional components of the active site: a reactive diiron centre, an amine as a proton relay and, for the first time, a one-electron redox module. By virtue of the synthetic redox cofactor, $[1]^{2+}$ exhibits unique reactivity towards hydrogen and CO. In the presence of excess oxidant and base, H_2 oxidation by $[1]^{2+}$ is catalytic.

Hydrogenase enzymes catalyse the interconversion of H_2 with protons and reducing equivalents. Mimicking the reactivity of these enzymes by means of active-site models is currently of interest because these catalysts rely on inexpensive first-row transition metals and the potential of hydrogen as an energy carrier[1–6]. The hydrogenases function by combining cofactors that couple acid–base and redox reactions mediated by the diiron dithiolate core and its cofactors (Fig. 1). The amine cofactor ('azadithiolate') relays protons to and from the distal Fe. A 4Fe–4S cluster is attached to the 2Fe–2S core through a single cysteinate residue and provides one redox equivalent to complement the one-electron couple for the diiron dithiolate core. The active site has been characterized in two functional states that differ by one electron: one state, H_{red}, poised to reduce protons and the other, H_{ox}, poised to oxidize H_2 (refs 7,8).

Over the last decade, efforts at functional modelling of the H_{red} state with these systems have identified electrocatalysts for proton reduction that operate via hydrides bound to an apical position on one Fe centre[9–11]. The amine cofactor (adt)[12], for which there is increasing direct biophysical evidence[13,14], plays an important role in proton reduction catalysis[15]. Several models for the H_{ox} state have also been reported[16], the defining feature of which is their mixed valency. Models for H_{ox}, even those containing azadithiolates[17–19],

*Correspondence and requests for materials should be addressed to T.B.R. rauchfuz@uiuc.edu.

Author contributions
All experiments were conducted by J.M.C., with input from T.B.R. The manuscript was written jointly by T.B.R. and J.M.C.

Additional information
The authors declare no competing financial interests. Supplementary information accompanies this paper at www.nature.com/naturechemistry. Reprints and permission information is available online at http://www.nature.com/reprints.

react only slowly with H_2 under forcing conditions[17]. Recently, we reported that the addition of mild oxidant to solutions of H_{ox} models allows for facile oxidation of H_2 (ref. 18). This finding suggests that functional models of the H_{ox} state require the presence of both an azadithiolate cofactor as well as a suitably tuned redox cofactor. Synthetic redox cofactors[11,20–22] that are intended to mimic the role of the 4Fe–4S cluster have been incorporated into models, but they have exhibited no functional role before this work.

In designing a model featuring both acid–base and redox functionality, we sought a synthetic cofactor with the following biologically inspired properties: (i) mild redox couple closer to the H_2/H^+ couple, in the range −0.3 to −1 V versus the ferrocene/ferrocinium couple ($Fc^{+/0}$); (ii) chemical inertness, so that reactions would be localized at the Fe_2 core; and (iii) a ligand that would bind tightly to a single Fe centre. Ferrocene-derived ligands seemed an obvious choice due to their chemical inertness and their one-electron redox chemistry[23]. Although many ferrocenyl phosphine ligands are known, in almost all cases—most famously dppf—the ferrocene serves simply as an inert scaffold and does not engage in redox. Ferrocenyl phosphines do undergo redox, but only at highly positive potentials, usually >0 V versus $Fc^{+/0}$ (640 mV versus normal hydrogen electrode, NHE)[24]. Such high potentials are incompatible with hydrogenase mimics because they would oxidize the H_{ox} state, inducing binding of the amine cofactor to Fe. Decamethylferrocene (Fc*), $E_{1/2}$ = −550 mV versus $Fc^{+/0}$ (187 mV versus NHE), represents an attractive alternative to ferrocene, although it has not been incorporated into monodentate redox-active ligands[25]. A potential problem with Fc* is its steric bulk, which may discourage coordination. We therefore targeted $Cp^*Fe(C_5Me_4CH_2PEt_2)$ (*FcP**, $Cp^* = C_5Me_5$), where the highly basic trialkylphosphine substituent is separated from the redox agent by a methylene spacer. As we describe in the following, incorporating *FcP** into a model for the H_{ox} state of [FeFe]-hydrogenase enables the binding of substrates in a manner not previously observed.

Results and discussion

Preparation of *FcP** and the reduced active site model

The redox-active ligand *FcP** was accessed readily from a procedure involving the concomitant formation of the C–P bond and the generation of an anionic tetraalkylcyclopentadienyl ligand. Commercially available C_5Me_5H was thus converted in one pot to $LiC_5Me_4CH_2PEt_2$ (ref. 26). This salt was treated with $[Cp^*FeCl]_2$ generated *in situ* to give *FcP** in ~55% isolated yield as a bright yellow solid (Fig. 2)[27]. In CH_2Cl_2 solution (0.1 M $NBu_4BAr^F_4$, Ar^F = 3,5-$C_6H_3(CF_3)_2$), *FcP** reversibly oxidizes with $E_{1/2}$ = −591 mV. Given the mildness of its redox potential, *FcP** is well suited to explore redox-induced reactions that occur near the H^+/H_2 couple[28].

*FcP** was installed on a diiron azadithiolato platform by reaction with $Fe_2[(SCH_2)_2NBn](CO)_4$(dppv), which is known to undergo monosubstitution by basic ligands (dppv = *cis*-$C_2H_2(PPh_2)_2$, Bn = CH_2Ph)[29]. The resulting complex $Fe_2[(SCH_2)_2NBn](CO)_3$(*FcP**)(dppv) (**1**) was isolated in analytical purity and exhibits spectroscopic properties similar to those of the simpler model $Fe_2[(SCH_2)_2NBn](CO)_3(PMe_3)$(dppv) (**2**), which features a diphosphine and monophosphine ligand on separate Fe centres. The oxidation states of the Fe centres in **1** are *Fe(II)*Fe(I)Fe(I). Treatment of **1** with $H(OEt_2)_2BAr^F_4$ gave the hydride $[\mathbf{1}H]^+$ (Fig. 3). The Fe oxidation states within $[\mathbf{1}H]^+$ are *Fe*(II)Fe(II)Fe(II). Overall, the spectroscopic properties of **1** and $[\mathbf{1}H]^+$ are very similar to those for **2** and $[\mathbf{2}H]^+$, respectively.

Redox states of $[Fe_2[(SCH_2)_2NBn](CO)_3$(*FcP**)(dppv)$]^{n+}$

The influence of the *FcP** ligand on the properties of the diiron dithiolate was revealed through a combination of electrochemical and spectroscopic measurements. Because H_2 is a

weakly basic ligand, these experiments used the weakly basic aryl borate anion BAr^{F-}_4, which does not compete with potential substrates. In dichloromethane solution, the cyclic voltammetry of **1** exhibits two reversible one-electron redox events (electrolyte: 0.1 M $NBu_4BAr^F_4$), the first at −700 mV, comparable to the $[\mathbf{2}]^{0/+}$ couple at −643 mV. For $[\mathbf{1}]^+$, but not for $[\mathbf{2}]^+$, a second oxidation was observed at −393 mV versus $Fc^{0/+}$. The localization of the oxidation changes in $[\mathbf{1}]^{n+}$ was probed by monitoring the titration of **1** with the oxidant $FcBAr^F_4$ using Fourier-transform infrared (FT-IR) spectroscopy (Fig. 4). The addition of 1 equiv. of $FcBAr^F_4$ to a CH_2Cl_2 solution of **1** resulted in a ~60 cm^{-1} shift in the two ν_{CO} bands to higher energy. The IR spectrum of $[\mathbf{1}]^+$ closely matches that for $[\mathbf{2}]^+$ (ref. 30). Thus, one-electron oxidation results in the formation of a normal H_{ox}-like mixed valence state[16,19,31,32]. Perhaps because of the steric bulk of the *FcP** ligand, the salt $[\mathbf{1}]BAr^F_4$ is noticeably more stable than $[\mathbf{2}]BAr^F_4$ (ref. 17). For example, solid $[\mathbf{1}]BAr^F_4$ can be precipitated and handled at room temperature. Addition of a second equivalent of $FcBAr^F_4$ to a solution of $[\mathbf{1}]BAr^F_4$ shifted υ_{CO} by only ~4 cm^{-1}, consistent with oxidation away from the diiron centre and hence localized at *FcP** (Fig. 4). Thus, the oxidation states in $[\mathbf{1}]^{2+}$ are *Fe(III)*Fe(II)Fe(I). The $[FcP^*]^{+/0}$ couple shifts by 200 mV upon coordination, reflecting both the inductive influence of the appended diiron unit and ion pairing effects[33,34]. The electronic interaction between the diiron subunit and the appended ferrocenyl ligand is reminiscent of the coupling between the diiron subunit and the appended 4Fe–4S cluster in the H cluster[35,36].

The assignments of oxidation state from the changes in the IR spectrum are supported by electron paramagnetic resonance (EPR) spectroscopic measurements. The room-temperature EPR spectrum of $[\mathbf{1}]^+$ is similar to that reported for the related $[\mathbf{2}]^+$ (ref. 37): the axial spectrum exhibits large hyperfine coupling to a pair of ^{31}P centres with $A_z(^{31}P)$ = 79.9 MHz. This pattern indicates that the unpaired electron resides mostly on the Fe atom distal *FcP** and suggests a formal assignment of $[\mathbf{1}]^+$ as (*FcP**)$(CO)_2Fe^{II}$ (μ-$SR)_2Fe^I$ (dppv)(CO). The doubly oxidized species $[\mathbf{1}]^{2+}$ is, however, EPR-silent from room temperature to 110 K (in 50/50 toluene/CH_2Cl_2 glass). A solution of a 1:1 mixture of $[\mathbf{2}]^+$ and $[Fc^*]^+$ exhibits a normal H_{ox} EPR spectrum. Variable-temperature magnetic susceptibility measurements indicate that $[\mathbf{1}]^+$ has a single unpaired electron and $[\mathbf{1}]^{2+}$ has two unpaired electrons. The absence of an EPR signal for $[\mathbf{1}]^{2+}$ may result from the two spins of $[\mathbf{1}]^{2+}$ undergoing fast relaxation at 110 K. Indeed, at very low temperatures (4.5 K), a very broad signal is observed at g ≈ 1.65, consistent with the presence of a fast-relaxing triplet state.

Reactions of $Fe_2[(SCH_2)_2NBn](CO)_3$(*FcP**)$(dppv)]^{n+}$ with CO and H_2

Having established that the model can be poised in three different oxidation states, **1**, $[\mathbf{1}]^+$ and $[\mathbf{1}]^{2+}$, we investigated how the oxidized states interact with CO and H_2, two well studied substrates for hydrogenases[38–41]. As shown below, the *FcP** ligand strongly influences the reactivity of the diiron centre. Although $[\mathbf{1}]^+$ does not bind CO at room temperature, solutions of $[\mathbf{1}]^{2+}$ visibly bind CO at room temperature. Thus, in the presence of CO, purple solutions of $[\mathbf{1}]^{2+}$ become orange, indicative of intramolecular redox to yield the all ferrous complex, that is, *Fe*(III)Fe(II)Fe(I) → Fe(II)Fe(II)Fe(II)CO. The reversible binding of CO to $[\mathbf{1}]^{2+}$ can be monitored by IR as well as ^{31}P NMR spectroscopies. With 1 atm of CO, solutions of $[\mathbf{1}]^{2+}$ in dichloromethane show the formation of ~50% of the adduct $[\mathbf{1}CO]^{2+}$ (Fig. 5). At lower temperatures the binding of CO is quantitative, leading to diamagnetic solutions of $[\mathbf{1}(CO)]^{2+}$ that exhibit well-resolved ^{31}P NMR spectra consistent with a single, unsymmetrical isomer. One likely explanation for this interesting reactivity is that CO binding induces electron transfer to the pendant ferrocenium, resulting in a switch from $Fe^{III}Fe^{II}Fe^I$ to $Fe^{II}Fe^{II}Fe^{II}$ (Fig. 3). Studies on the [FeFe]-hydrogenase from *Clostridium*

pasteurianum and *Desulfovibrio desulfuricans* indicate that CO binding induces partial oxidation of the distal Fe centre[42,43]. In the case of $[\mathbf{1}]^{2+}$, the effect is sufficiently strong that CO binding triggers full reduction of the ferrocenium centre.

Solutions of $[\mathbf{1}]^{2+}$, generated by treatment of **1** with 2 equiv. of $FcBAr^F_4$, visibly react on mixing with H_2 (1 atm) over the course of 1 h at 25 °C, a striking result. With previously described models, the reaction occurs only sluggishly and under harsh conditions in the absence of external oxidant[30]. The ^{1}H NMR spectrum of the resulting solution revealed signals at high field relative to tetramethylsilane (TMS), a region diagnostic of hydride products. Activation of H_2 is proposed to produce an ammonium hydride product. When the oxidation of H_2 by $[\mathbf{1}]^{2+}$ was conducted in the presence of the base P(*o*-tolyl)$_3$ (ref. 44), we observed clean formation of equimolar amounts of $[\mathbf{1}H]^+$ (see above) and phosphonium salt $[HP(o\text{-tolyl})_3]^+$ (Figs 3 and 5). Using D_2, we obtained exclusively the corresponding deuterated products $[\mathbf{1}D]^+$ and $[DP(o\text{-tolyl})_3]^+$, as established by ^{2}H NMR spectroscopy. The reaction of $[\mathbf{1}]^{2+}$ and H_2 in the presence of P(*o*-tolyl)$_3$ proceeds about four times faster than the previously reported reaction of $[\mathbf{2}]^+$ with H_2 in the presence of $Cp^*_2Fe^+$ and P(*o*-tolyl)$_3$ under identical conditions[18].

Whereas the cation $[\mathbf{2}]^+$ can only stoichiometrically activate H_2, the dication $[\mathbf{1}]^{2+}$ acts as a catalyst for the oxidation of H_2 in the presence of excess oxidant and excess base. We monitored the formation of $[HP(o\text{-tolyl})_3]^+$ on introducing an atmosphere of H_2 to a solution containing $[\mathbf{1}]^{2+}$, 6 equiv. of P(*o*-tolyl)$_3$ and excess oxidant (4 equiv. of $FcBAr^F_4$). After 5 h, ^{31}P NMR analysis confirmed the complete conversion of P(*o*-tol)$_3$ to $[HP(o\text{-tolyl})_3]^+$:

$$H_2 + 2\,P(o-\text{tolyl})_3 + 2\,Fc^+ \xrightarrow{\mathbf{1}} 2[\,HP(o-\text{tolyl})_3]^+ + 2\,Fc$$

When the analogous experiment was attempted using $[\mathbf{2}]^+$, with or without excess oxidant, the catalytic conversion of P(*o*-tolyl)$_3$ to $[HP(o\text{-tolyl})_3]^+$ was not observed. Catalytic turnover requires the deprotonation of the product hydride $[\mathbf{1}H]^+$ or, possibly, $[\mathbf{1}H]^{2+}$. Although the rate of hydrogen oxidation by $[\mathbf{1}]^{2+}$ is only 0.4 turnover/h, far slower than that for the enzyme itself, these results establish additional enabling properties conferred by the *FcP** functionality. Not only is the multifunctionalized diiron dithiolate capable of activating H_2, but its hydride also exhibits enhanced acidity upon oxidation, enabling catalytic turnover.

Conclusions

The experiments described above support the concept that the activation of H_2 by mixed valence diiron models benefits from the presence of a mild intramolecular oxidant[45], a function provided by an appended 4Fe–4S cluster in the [FeFe]-hydrogenases. Our experiments demonstrate that suitably modified ferrocenes can replicate the behaviour of 4Fe–4S clusters without their complications. Our approach shows that redox-complemented diiron systems display a number of properties not seen for simpler models such as redox-induced binding of CO, electronic coupling between the two $S = 1/2$ centres, and catalytic oxidation of H_2.

Given the importance of redox and especially proton-coupled electron transfer (PCET) in energy conversion schemes[46], the low potential redox properties of *FcP** are expected to be applicable to other themes in biomimetic catalysis.

Methods

All procedures were carried out using standard Schlenk techniques. Tetrahydrofuran (THF) was purified by distillation from Na/benzophenone. Other solvents were dried and degassed by passage through activated alumina and sparging with argon. IR spectra were recorded on a Perkin Elmer Spectrum 100. NMR spectra were recorded on a Varian Unity 500 MHz NMR spectrometer. Additional experimental procedures and details can be found in the Supplementary Information.

(Diethylphosphinomethyl)nonamethylferrocene (*FcP**)

$Li[C_5Me_4CH_2PEt_2]$ was prepared by slow addition of 22 ml of 2,3,4,5-tetramethylfulvene[26] solution (0.21 M in toluene) to 0.49 g (4.56 mmol) of $LiPEt_2$ in 100 ml of THF at −78 °C. The reaction mixture was allowed to warm to room temperature overnight, resulting in a pale yellow solution of $Li[C_5Me_4CH_2PEt_2]$. Finely ground $FeCl_2$ (0.578 g, 4.5 mmol) was added and stirred with 100 ml of THF for 2 h. The flask was then cooled to −78 °C and a pre-cooled solution of 0.648 g (7.1 mmol) of LiCp* in 60 ml THF was added by cannula over 10 min. The mixture was stirred at −30 °C until it turned olive green (about 1 h). The flask was then cooled to −78 °C, and the solution of $Li[C_5Me_4CH_2PEt_2]$ was added by cannula over the course of 1 h. The mixture was allowed to warm to room temperature and stirred overnight, during which time the solution became dark. Solvent was removed under vacuum. The resulting dark solid was extracted into 90 ml of pentane, which was filtered through Celite. The resulting yellow/orange filtrate was evaporated under vacuum and purified by chromatography on silica gel. Elution with 30/70 toluene/pentane yielded a fast-moving yellow band of decamethylferrocene; subsequent elution with 50/50 toluene/pentane yielded a second yellow band of desired product followed by a third yellow band of $(C_5Me_4CH_2PEt_2)_2Fe$ using 100% toluene. Yield: 1.05 g (55%). ^1H NMR (500 MHz, C_6D_6, 20 °C): δ 2.38 (s, 2H), 1.82 (s, 6H), 1.67 (s, 15H), 1.66 (s, 6H), 1.28 (m, 4H) 1.00 (dt, $J_{H\text{-}H}$ = 7 Hz, $J_{P\text{-}H}$ = 14.5 Hz, 6H). $^{31}P\{^1H\}$ NMR (202 MHz, C_6D_6, 20 °C): δ −18.4 (s). Anal. Calcd for $C_{29}H_{34}FeP$ (found): C, 69.56 (69.97); H, 9.49 (9.62).

$Fe_2(adt^{Bn})(CO)_3$(*FcP**)(dppv)

A 250 ml Schlenk flask was charged with a solution of 72 mg (0.17 mmol) of *FcP** and 142 mg (0.17 mmol) of $Fe_2(adt^{Bn})(CO)_4$(dppv) (ref. 17) in 100 ml toluene. The solution was photolysed in a Pyrex Schlenk tube at 450 nm using an light-emitting diode array. After ~12 h, the reaction was judged complete by IR spectroscopy, and solvent was removed under vacuum to give 182 mg (87%) product. ^1H NMR (500 MHz, C_6D_6, 20 °C): δ 8.07–7.93 (m, 6H), 7.48–7.39 (m, 6H), 7.30–7.09 (m, 13H), 6.74 (d, $J_{P\text{-}H}$ = 5 Hz, 2H), 3.05 (d, $J_{H\text{-}H}$ = 5 Hz, 2H), 3.00 (s, 1H), 2.77 (d, $J_{H\text{-}H}$ = 10 Hz), 1.98 (d, $J_{H\text{-}H}$ = 5 Hz), 1.72 (s, 6H), 1.72 (s, 6H), 1.69 (m, overlapping, ~4H), 1.66 (s, 15H), 1.04 (dt, $J_{P\text{-}H}$ = 15 Hz, $J_{H\text{-}H}$ = 7 Hz, 6H). $^{31}P\{^1H\}$ NMR (162 MHz, C_6D_6, 20 °C): δ 93.9 (s, 2P), 59.9 (s, 1P). IR (CH_2Cl_2): ν_{CO} = 2,022 (w), 1,958 (s), 1,945 (m), 1,907 (s), 1,897 (s), 1,881 (m) cm^{-1}. Anal. Calcd for $C_{62}H_{73}Fe_3NO_3P_3S_2$ (found): C, 62.34 (62.86); H, 6.13 (6.21); N, 1.01(1.16).

$[HFe_2(adt^{Bn})(CO)_3$(*FcP**)(dppv)$]BAr^F_4$

Via 1 and $H(OEt_2)_2BAr^F_4$—In a Schlenk flask, a solution of 15 mg (12.5 mmol) of **1** in 2 ml CH_2Cl_2 was treated with a solution of 12.66 mg (12.5 μmol) $H(OEt_2)_2BAr^F_4$ in 5 ml CH_2Cl_2. The resulting solution was stirred for 30 min, during which time the solution colour changed from brown to red-orange. The product was precipitated by adding 25 ml hexanes. The resulting red-brown coloured solid was washed with small portions of hexane and dried under vacuum. Yield: 22 mg (85% yield) of [**1**H]BAr^F_4. ^{31}P NMR (202 MHz, CD_2Cl_2, 20

°C): δ 93.2 (dd, $J_{P\text{-}P}$ = 5 Hz, 4 Hz, 1P), 89.1 (d, $J_{P\text{-}P}$ = 4 Hz, 1P), 54.3 (d, $J_{P\text{-}P}$ = 5 Hz, 1P); ^{1}H NMR (500 MHz, CD_2Cl_2, 20 °C): δ −15.33 (ddd, $J_{P\text{-}H}$ = 22 Hz, 19.3 Hz, 3.8 Hz). IR (CH_2Cl_2): ν_{CO} = 2,023 (m) and 1,973 (s) cm^{-1}. Anal. Calcd for $C_{94}H_{85}BF_{24}Fe_3NO_3P_3S_2$ (found): C, 54.59 (54.92); H, 4.14 (4.09); N 0.68 (0.83).

Via H_2 and [1]$^{2+}$—In a Schlenk flask, 15 mg (12.5 μmol) of **1**, 3.6 mg (12.5 μmol) of P(*o*-tol)$_3$ and 26.2 mg (25 μmol) of $FcBAr^F_4$ were dissolved in 5 ml CH_2Cl_2, resulting in a deep purple solution. Hydrogen was then bubbled through the solution, which changed from deep purple to red-orange. IR spectroscopy showed that conversion to [**1**H]$^+$ was complete within 1 h. The IR, ^{31}P NMR, and ^{1}H NMR spectra of the product matched those for [**1**H]BAr^F_4 prepared from treatment of **1** with $H(OEt_2)_2BAr^F_4$ as above.

[Fe_2(adt^{Bn})(CO)$_4$(*FcP**)(dppv)][BAr^F_4]$_2$, [1(CO)][BAr^F_4]$_2$

In a Schlenk flask, a solution was prepared of 15 mg (12.5 μmol) of **1** and 26.2 mg (25 μmol) of $FcBAr^F_4$ in 5 ml CH_2Cl_2. CO was then bubbled through the solution, which changed colour from deep purple to orange within seconds. Solution IR spectroscopy showed new ν_{CO} bands at 2,077, 2,051 and 2,018 cm^{-1}. On purging with dry Ar, these bands disappeared, restoring the original colour and IR spectrum of [**1**]$^{2+}$. To probe the reaction by ^{31}P NMR spectroscopy, a J. Young tube was charged with 4.2 mg (3.5 μmol) of **1**, 7.3 mg (7 μmol) $FcBAr^F_4$ and 0.75 ml CD_2Cl_2. The ^{31}P NMR spectrum showed no resonances. The tube was pressurized with CO (2 atm) and cooled to −50 °C, resulting in a colour change from purple through orange to lime-green. ^{31}P NMR (202 MHz, CD_2Cl_2, −50 °C): δ 68.6 (dd, $J_{P\text{-}P}$ = 10 Hz, 6 Hz, 1P), 68.1 (d, $J_{P\text{-}P}$ = 6 Hz, 1P), 39.1 (broad, 1P).

Supplementary Material

Refer to Web version on PubMed Central for supplementary material.

Acknowledgments

This research was supported by the National Institutes of Health. The authors thank M. Nilges for assistance with EPR and M. Olsen for helpful discussions.

References

1. Bullock, RM. Catalysis Without Precious Metals. Wiley-VCH; 2010.
2. Felton GAN, et al. Review of electrochemical studies of complexes containing the Fe_2S_2 core characteristic of [FeFe]-hydrogenases including catalysis by these complexes of the reduction of acids to form dihydrogen. J. Organomet. Chem. 2009; 694:2681–2699.
3. Gloaguen F, Rauchfuss TB. Small molecule mimics of hydrogenase: hydrides and redox. Chem. Soc. Rev. 2009; 38:100–108. [PubMed: 19088969]
4. Hu XL, Brunschwig BS, Peters JC. Electrocatalytic hydrogen evolution at low overpotentials by cobalt macrocyclic glyoxime and tetraimine complexes. J. Am. Chem. Soc. 2007; 129:8988–8998. [PubMed: 17602556]
5. Lee CH, Dogutan DK, Nocera DG. Hydrogen generation by hangman metalloporphyrins. J. Am. Chem. Soc. 2011; 133:8775–8777. [PubMed: 21557608]
6. Rakowski DuBois M, DuBois DL. Development of molecular electrocatalysts for CO_2 reduction and H_2 production/oxidation. Acc. Chem. Res. 2009; 42:1974–1982. [PubMed: 19645445]
7. Fontecilla-Camps JC, Volbeda A, Cavazza C, Nicolet Y. Structure/function relationships of [NiFe]- and [FeFe]-hydrogenases. Chem. Rev. 2007; 107:4273–4303. [PubMed: 17850165]

8. Tard C, Pickett CJ. Structural and functional analogues of the active sites of the [Fe]-, [NiFe]-, and [FeFe]-hydrogenases. Chem. Rev. 2009; 109:2245–2274. [PubMed: 19438209]
9. Capon J-F, Gloaguen F, Pétillon FY, Schollhammer P, Talarmin J. Electron and proton transfers at diiron dithiolate sites relevant to the catalysis of proton reduction by the [FeFe]-hydrogenases. Coord. Chem. Rev. 2009; 253:1476–1494.
10. Barton BE, Rauchfuss TB. Terminal hydride in [FeFe]-hydrogenase model has lower potential for H_2 production than the isomeric bridging hydride. Inorg. Chem. 2008; 47:2261–2263. [PubMed: 18333613]
11. Tard C, et al. Synthesis of the H-cluster framework of iron-only hydrogenase. Nature. 2005; 433:610–614. [PubMed: 15703741]
12. Ezzaher S, et al. Electron-transfer-catalyzed rearrangement of unsymmetrically substituted diiron dithiolate complexes related to the active site of the [FeFe]- hydrogenases. Inorg. Chem. 2007; 46:9863–9872. [PubMed: 17941631]
13. Silakov A, Wenk B, Reijerse E, Lubitz W. ^{14}N HYSCORE investigation of the H-cluster of [FeFe] hydrogenase: evidence for a nitrogen in the dithiol bridge. Phys. Chem. Chem. Phys. 2009; 11:6592–6599. [PubMed: 19639134]
14. Erdem ÖF, et al. A model of the [FeFe] hydrogenase active site with a biologically relevant azadithiolate bridge: a spectroscopic and theoretical investigation. Angew. Chem. Int. Ed. 2011; 50:1439–1443.
15. Barton BE, Olsen MT, Rauchfuss TB. Aza- and oxadithiolates are probable proton relays in functional models for the [FeFe]-hydrogenases. J. Am. Chem. Soc. 2008; 130:16834–16835. [PubMed: 19053433]
16. Thomas CM, Liu T, Hall MB, Darensbourg MY. Series of mixed valent Fe(ii)Fe(i) complexes that model the H_{ox} state of [FeFe] hydrogenase: redox properties, density-functional theory investigation, and reactivities with extrinsic CO. Inorg. Chem. 2008; 47:7009–7024. [PubMed: 18597449]
17. Olsen MT, Barton BE, Rauchfuss TB. Hydrogen activation by biomimetic diiron dithiolates. Inorg. Chem. 2009; 48:7507–7509. [PubMed: 19603776]
18. Camara JM, Rauchfuss TB. Mild redox complementation enables H_2 activation by [FeFe]-hydrogenase models. J. Am. Chem. Soc. 2011; 133:8098–8101. [PubMed: 21548619]
19. Justice AK, et al. Redox and structural properties of mixed-valence models for the active site of the [FeFe]-hydrogenase: progress and challenges. Inorg. Chem. 2008; 47:7405–7414. [PubMed: 18620387]
20. Liu Y-C, Lee C-H, Lee G-H, Chiang M-H. Influence of a redox-active phosphane ligand on the oxidations of a diiron core related to the active site of Fe-only hydrogenase. Eur. J. Inorg. Chem. 2011; 2011:1155–1162.
21. Zeng X, Li Z, Xiao Z, Wang Y, Liu X. Using pendant ferrocenyl group(s) as an intramolecular standard to probe the reduction of diiron hexacarbonyl model complexes for the sub-unit of [FeFe]-hydrogenase. Electrochem. Commun. 2010; 12:342–345.
22. Si Y, et al. Non-innocent bma ligand in a dissymetrically disubstituted diiron dithiolate related to the active site of the [FeFe] hydrogenases. J. Inorg. Biochem. 2010; 104:1038–1042. [PubMed: 20547420]
23. Connelly NG, Geiger WE. Chemical redox agents for organometallic chemistry. Chem. Rev. 1996; 96:877–922. [PubMed: 11848774]
24. Stepnicka, P. Ferrocenes. Wiley; 2008.
25. Aranzaes JR, Daniel MC, Astruc D. Metallocenes as references for the determination of redox potentials by cyclic voltammetry—permethylated iron and cobalt sandwich complexes, inhibition by polyamine dendrimers, and the role of hydroxy-containing ferrocenes. Can. J. Chem. 2006; 84:288–299.
26. Döring S, Erker G. Preparation of 1,2,3,4-tetramethylpentafulvene by hydride anion abstraction from lithium pentamethylcyclopentadienide employing trityl chloride. Synthesis. 2001:43–45.
27. Herberich GE, Gaffke A, Eckenrath HJ. Cyclopentadienyl(pentamethylcyclopentadienyl) iron derivatives. A new and highly selective synthesis. Organometallics. 1998; 17:5931–5932.

28. Felton GAN, Glass RS, Lichtenberger DL, Evans DH. Iron-only hydrogenase mimics. Thermodynamic aspects of the use of electrochemistry to evaluate catalytic efficiency for hydrogen generation. Inorg. Chem. 2006; 45:9181–9184. [PubMed: 17083215]
29. Justice AK, et al. Chelate control of diiron(I) dithiolates relevant to the Fe-only hydrogenase active site. Inorg. Chem. 2007; 46:1655–1664. [PubMed: 17279743]
30. Olsen MT, Rauchfuss TB, Wilson SR. Role of the azadithiolate cofactor in models for [FeFe]-hydrogenase: novel structures and catalytic implications. J. Am. Chem. Soc. 2010; 132:1733–1740.
31. Justice AK, Rauchfuss TB, Wilson SR. Unsaturated, mixed valence diiron dithiolate model for the H_{ox} state of the [FeFe]-hydrogenase. Angew. Chem. Int. Ed. 2007; 46:6152–6154.
32. Liu T, Darensbourg MY. A mixed-valent, Fe(ii)Fe(i), diiron complex reproduces the unique rotated state of the [FeFe]-hydrogenase active site. J. Am. Chem. Soc. 2007; 129:7008–7009. [PubMed: 17497786]
33. Geiger WE, Barrière F. Organometallic electrochemistry based on electrolytes containing weakly-coordinating fluoroarylborate anions. Acc. Chem. Res. 2010; 43:1030–1039. [PubMed: 20345126]
34. Diallo AK, Daran J-C, Varret F, Ruiz J, Astruc D. How do redox groups behave around a rigid molecular platform? Hexa(ferrocenylethynyl)benzenes and their 'electrostatic' redox chemistry. Angew. Chem. Int. Ed. 2009; 48:3141–3145.
35. Roseboom W, Lacey AL, Fernandez VM, Hatchikian EC, Albracht SPJ. The active site of the [FeFe]-hydrogenase from *Desulfovibrio desulfuricans*. II. Redox properties, light sensitivity and CO-ligand exchange as observed by infrared spectroscopy. J. Biol. Inorg. Chem. 2006; 11:102–118. [PubMed: 16323019]
36. Silakov A, Kamp C, Reijerse E, Happe T, Lubitz W. Spectroelectrochemical characterization of the active site of the [FeFe] hydrogenase HydA1 from *Chlamydomonas reinhardtii*. Biochemistry. 2009; 48:7780–7786. [PubMed: 19634879]
37. Justice AK, et al. Diiron dithiolato carbonyls related to HoxCO state of [FeFe]- hydrogenase. J. Am. Chem. Soc. 2008; 130:5293–5301. [PubMed: 18341276]
38. Parkin A, Cavazza C, Fontecilla-Camps JC, Armstrong FA. Electrochemical investigations of the interconversions between catalytic and inhibited states of the [FeFe]-hydrogenase from *Desulfovibrio desulfuricans*. J. Am. Chem. Soc. 2006; 128:16808–16815. [PubMed: 17177431]
39. Roseboom W, De Lacey AL, Fernandez VM, Hatchikian EC, Albracht SPJ. The active site of the FeFe -hydrogenase from *Desulfovibrio desulfuricans*. II. Redox properties, light sensitivity and CO-ligand exchange as observed by infrared spectroscopy. J. Biol. Inorg. Chem. 2006; 11:102–118. [PubMed: 16323019]
40. Vincent KA, Parkin A, Armstrong FA. Investigating and exploiting the electrocatalytic properties of hydrogenases. Chem. Rev. 2007; 107:4366–4413. [PubMed: 17845060]
41. De Lacey AL, Fernández VM, Rousset M, Cammack R. Activation and inactivation of hydrogenase function and the catalytic cycle: spectroelectrochemical studies. Chem. Rev. 2007; 107:4304–4330. [PubMed: 17715982]
42. Telser J, Benecky MJ, Adams MWW, Mortenson LE, Hoffman BM. An electron-paramagnetic-resonance and electron nuclear double-resonance investigation of the carbon-monoxide binding to hydrogenase-I (bidirectional) from *Clostridium pasteurianum* W5. J. Biol. Chem. 1986; 261:3536–3541. [PubMed: 3005291]
43. Silakov A, Reijerse EJ, Albracht SPJ, Hatchikian EC, Lubitz W. The electronic structure of the H-cluster in the [FeFe]-hydrogenase from *Desulfovibrio desulfuricans*: A Q-band ^{57}Fe-ENDOR and HYSCORE study. J. Am. Chem. Soc. 2007; 129:11447–11458. [PubMed: 17722921]
44. Ullrich M, Lough AJ, Stephan DW. Dihydrogen activation by B(*p*-$C_6F_4H)_3$ and phosphines. Organometallics. 2010; 29:3647–3654.
45. Greco C, De Gioia L. A theoretical study on the enhancement of functionally relevant electron transfers in biomimetic models of [FeFe]-hydrogenases. Inorg. Chem. 2011; 50:6987–6995. [PubMed: 21728321]
46. Hammes-Schiffer S. Theory of proton-coupled electron transfer in energy conversion processes. Acc. Chem. Res. 2009; 42:1881–1889. [PubMed: 19807148]

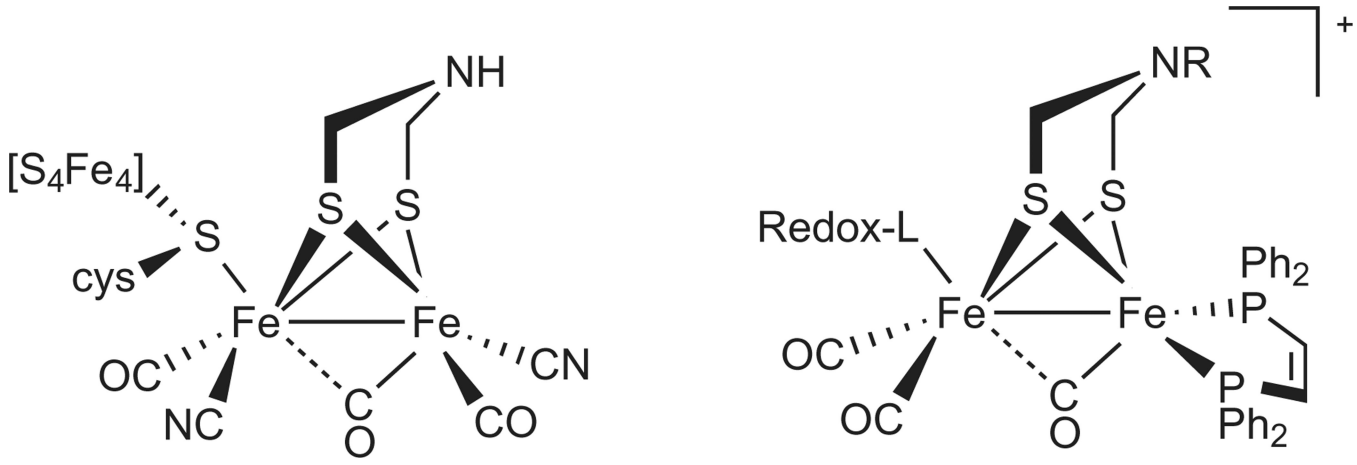

Figure 1. Structure of active site for the [FeFe]-hydrogenase and its model

Both structures contain functionality dedicated to substrate binding as well as the management of redox equivalents and proton equivalents. As shown on the left, the active site consists of a $Fe_2(CO)_3(CN)_2$ centre bridged by the Brønsted-basic azadithiolate (SCH_2NHCH_2S) cofactor. The redox cofactor, a 4Fe–4S cluster, is attached to a single Fe centre. Substrate binding occurs at the Fe centre distal to the 4Fe–4S cluster and adjacent to the basic amine. The proposed model complex also features an $Fe_2(CO)_3$ centre bridged by a basic azadithiolate with an alkyl groups R in place of H. A redox-active ligand (Redox-L) simulates the function of the 4Fe–4S cluster, and the phosphine ligands simulate the coordinated cyanides.

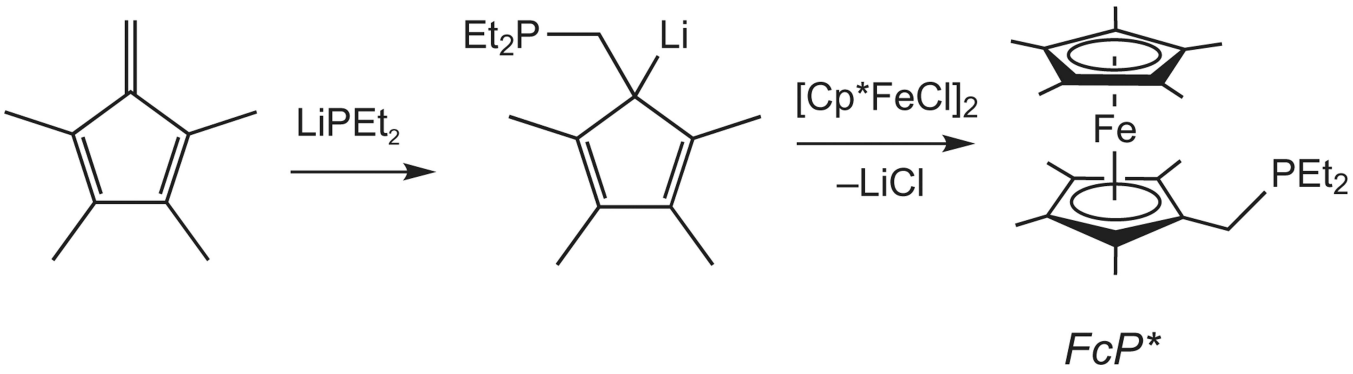

Figure 2. Synthesis of *FcP**

The route starts with the formation of the C–P bond and generation of $LiC_5Me_4CH_2PEt_2$. Combining this organolithium reagent with "$(C_5Me_5)FeCl$" gives *FcP**.

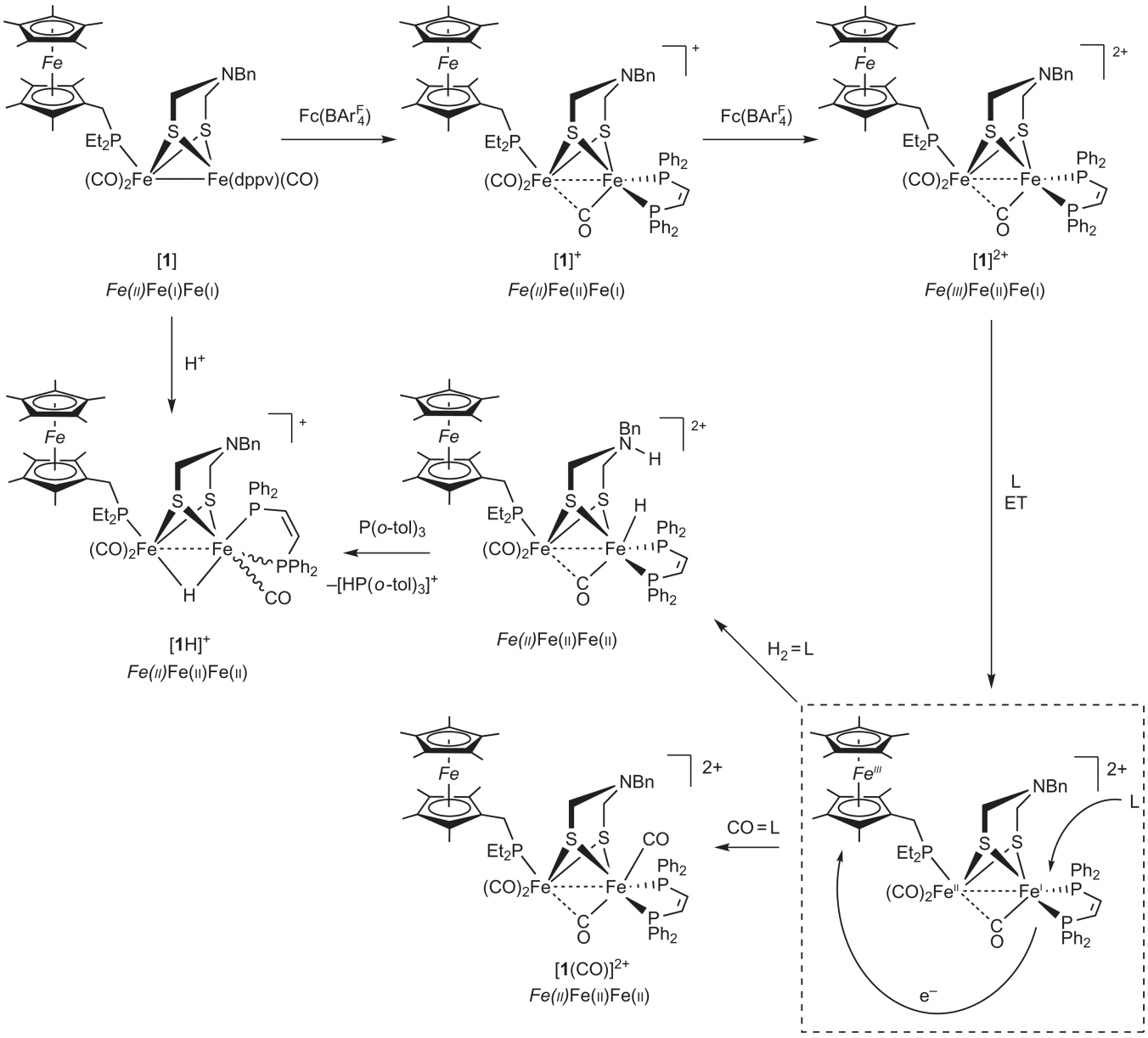

Figure 3. Summary of reactions observed for $[1]^{2+}$ with CO and H_2

Compound numbering and relevant oxidation states are shown, using italics for the ferrocenyl iron centre. The starting compound **1** is in a fully reduced state. Initial oxidation of **1** is localized on the diiron core as shown by FT-IR and EPR measurements. The second oxidation (to $[\mathbf{1}]^{2+}$) converts the *FcP** centre from ferrous to ferric. Reactions of $[\mathbf{1}]^{2+}$ with H_2 and with CO involve substrate binding coupled to intramolecular electron-transfer (ET) from the diiron subunit to the oxidized *FcP** ligand.

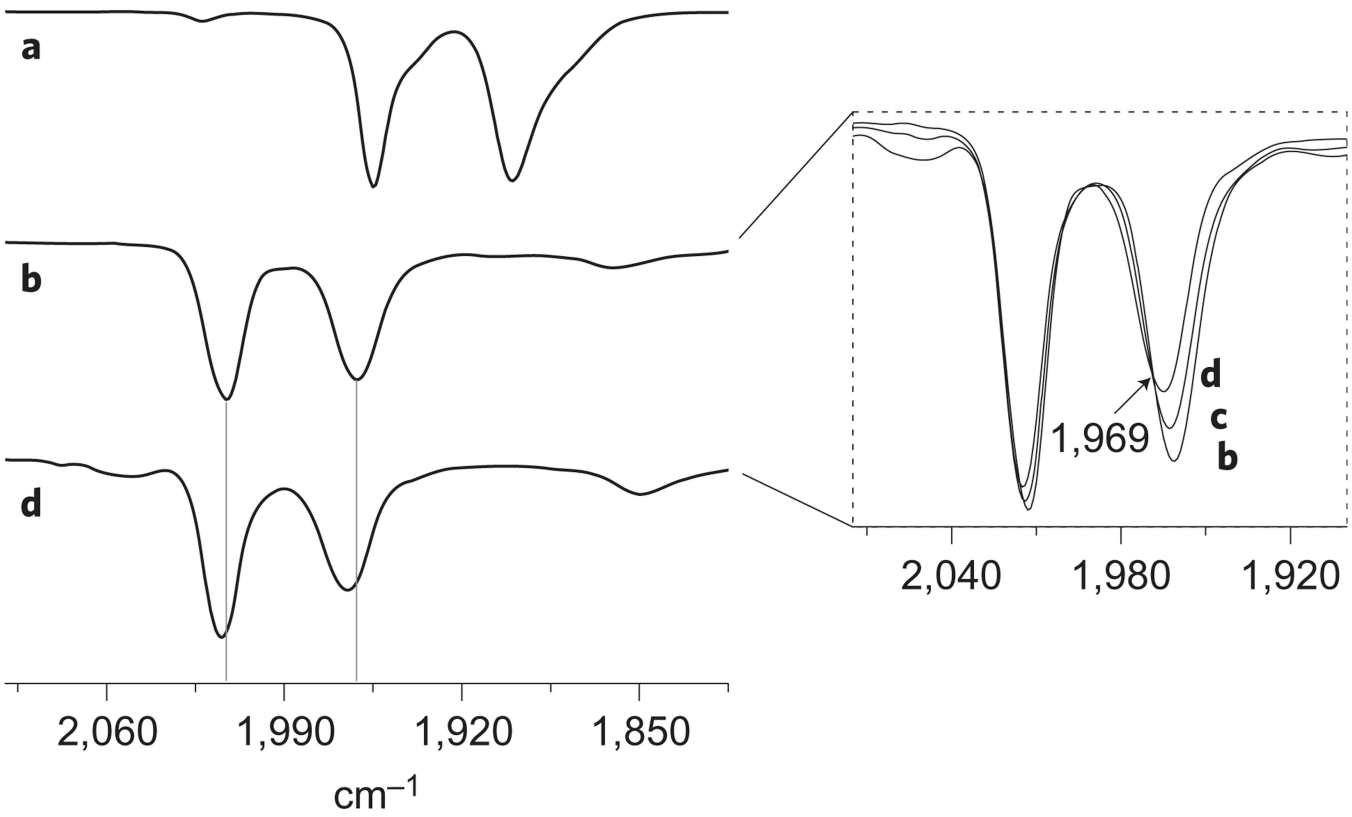

Figure 4. Infrared spectra probing the localization of the two one-electron oxidations of the reduced model [1]

a–d, Titration of $FcBAr^F_4$ into a CH_2Cl_2 solution of **1** monitored by solution IR spectroscopy: [**1**] (**a**), [**1**] + 1 equiv. $FcBAr^F_4$ (**b**), [**1**] + 1.5 equiv. $FcBAr^F_4$ (**c**), [**1**] + 2 equiv. $FcBAr^F_4$ (**d**). On conversion of $[\mathbf{1}]^+$ to $[\mathbf{1}]^{2+}$, an isosbestic point is observed at 1,969 cm^{-1}.

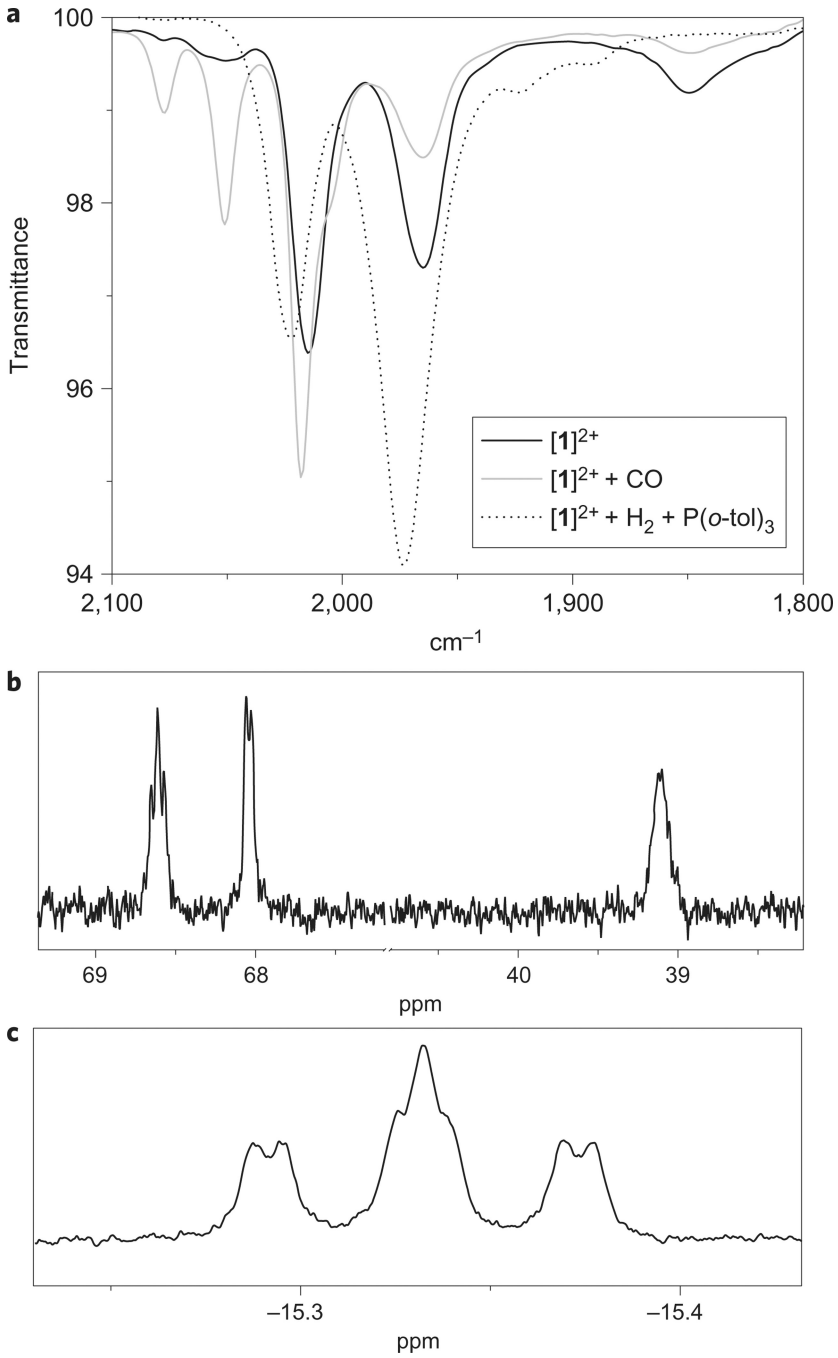

Figure 5. Spectroscopic evidence confirming the reactions of $[\mathbf{1}]^{2+}$ with known hydrogenase substrates H_2 and CO

a, IR spectra of dichloromethane solutions of $[\mathbf{1}]^{2+}$ before and after treatment with CO (1 atm) and H_2 (1 atm) at 25 °C. In each case, the formation of a new carbonyl-containing species is indicated by the appearance of new ν_{CO} bands on the addition of the indicated substrate. **b**, ^{31}P NMR spectrum (202 MHz, CD_2Cl_2) of $[\mathbf{1}(CO)]^{2+}$ at −60 °C showing the conversion of the ^{31}P NMR-silent paramagnetic $[\mathbf{1}]^{2+}$ to the ^{31}P NMR-active diamagnetic adduct $[\mathbf{1}(CO)]^{2+}$. **c**, ^{1}H NMR (500 MHz, CD_2Cl_2) hydride resonance of $[\mathbf{1}H]^{+}$ obtained from treatment of $[\mathbf{1}]^{2+}$ with H_2 and P(*o*-tol)$_3$.